Japanese Journal of Applied Physics

The Japan Society of Applied Physics

PROGRESS REVIEW

Novel energy-efficient designs of vertical-cavity surface emitting lasers for the next generations of photonic systems

To cite this article: Si-Cong Tian *et al* 2022 *Jpn. J. Appl. Phys.* **61** SK0801

Japanese Journal of Applied Physics 61, SK0801 (2022) **PROGRESS REVIEW**
https://doi.org/10.35848/1347-4065/ac65d9

Novel energy-efficient designs of vertical-cavity surface emitting lasers for the next generations of photonic systems

Si-Cong Tian[1,2*], Mansoor Ahamed[1,3], Gunter Larisch[1,2], and Dieter Bimberg[1,2*]

[1]Bimberg Chinese-German Center for Green Photonics, Changchun Institute of Optics, Fine Mechanics, and Physics, Chinese Academy of Sciences, Changchun 130033, People's Republic of China
[2]Center of Nanophotonics, Institute of Solid State Physics, Technische Universität Berlin, Berlin D-10632, Germany
[3]The University of Chinese Academy of Sciences, Beijing 100049, People's Republic of China

*E-mail: tiansicong@ciomp.ac.cn; bimberg@physik.tu-berlin.de

Received January 30, 2022; revised March 8, 2022; accepted April 8, 2022; published online June 16, 2022

High-speed vertical-cavity surface-emitting lasers (VCSELs) at different wavelengths present the backbone of high-speed optical links showing large bandwidth density. The state of the art of present designs of VCSELs is summarized, including driving conditions. Several novel approaches for the design of GaAs-based VCSELs and VCSEL arrays are reported, potentially leading, e.g. to lower power consumption, much larger single mode output and larger bandwidth. The first one is based on using the photon lifetime as a system sensitive optimization parameter. The second one reports for the first time details of a disruptively novel (patented) design based on oxidizing the apertures from multiple etched holes in varying arrangements and finally on multi-aperture designs in one device. These designs are essential for improving the energy-efficiency of modules by optimizing the interplay of electronic driver and photonic device.

1. Introduction

Since 2014 novel consumer and social media applications like Netflix, Block Chain,… not known to appear at the horizon until that time have led to a huge increase of internet traffic of ~60% year^{-1}, much more than originally predicted by companies like Cisco[1)] for the period 2017–2022. The electrical power consumption and cooling demand due to increased data traffic mostly inside data centers is presently exploding. New data centers have crossed the 500 MW level.

Introduction of 5 G and moving on to 6 G with their needs for big jumps in data rates are enablers for new services, like AI, and multiple automotive applications, we could not imagine a few years ago. The energy consumption by communication will additionally rise to an extent potentially not further tolerable. In order to avoid an introduction of limits for data consumption, the goals of present research have to be complemented by putting energy-efficiency of data traffic on all hierarchy levels including data centers as a primary goal, in addition to just hunting for increased bit rates at the expense of energy consumption.[2)]

Optical links utilizing GaAs-based vertical-cavity surface-emitting lasers (VCSELs), multimode fibers (MMFs), high-speed detectors, electronic drivers and amplifiers present the essential parts of data transmission, controlling the power budget.[3,4)] VCSELs exhibit low threshold currents, large quantum efficiency, modulation frequencies up to 25–30 GHz and a bit rate dependent energy consumption (power/bit).[5)] Increasing line rates under non-return-to-zero on–off keying (NRZ-OOK) modulation and 4-level pulse amplitude modulation (PAM-4) were demonstrated.[6,7)] In addition, single mode VCSELs using OOK transmitted data beyond 2000 m.[8)] By wavelength division multiplexing (WDM), the optical link capacity can be greatly increased.[9)] According to the Ethernet Roadmap 2018[10)] the bit rate shall reach 800 Gbit s^{-1} or 1.6 Tbit s^{-1} in 2022, under PAM-2 or PAM-4 modulation, respectively.

This paper is organized as follows:

In Sections 2 and 3, we will discuss selected results based on conventional design, and the speed limitations and optical link capacity of present VCSELs. In Sections 4–6, we will introduce novel designs approaches,

- system design adapted photon lifetime tuning,
- aperture formation from multiple etched holes and
- multiple aperture design

for the next generation of photonic systems based on GaAs VCSELs. The last Section will present a summary and an outlook on future developments including adaption to electronic CMOS drivers based on advanced ICs.

2. Design of conventional VCSELs

The schematics of a conventional VCSEL with aperture(s) on top of the active area is shown in Fig. 1.[11)] The active area of the VCSEL is based on quantum well (QW) or quantum dot (QD) gain layers and high-reflectance top and bottom distributed Bragg reflectors (DBRs). The oxide apertures, which are formed via a hot steam oxidation process, confine the current and guide the optical field in the device.

The modulation response of a VCSEL can be expressed by the transfer function

$$H(f) = C \times \frac{f_r^2}{\left(f_r^2 - f^2 + i\dfrac{\gamma}{2\pi}f\right)} \times \frac{1}{1 + i\dfrac{f}{f_P}}, \tag{1}$$

where C is a constant, f_r is the resonance frequency, γ is the damping and f_p is the parasitic cut-off frequency. The first part of Eq. (1) represents the intrinsic response and the second part of Eq. (1) represents the parasitic response.

The resonance frequency f_r, which is quantified by the D-factor, is increasing with the drive current I of the VCSEL,

$$f_r = D\sqrt{I - I_{\text{th}}} \tag{2}$$

where I_{th} is the threshold current, and

$$D = \frac{1}{2\pi}\sqrt{\frac{\eta_i \Gamma \nu_g}{qV_a} \cdot \frac{\partial g/\partial n}{\chi}}, \tag{3}$$

where η_i is the internal quantum efficiency, Γ is the optical confinement factor, ν_g is the photon group velocity, $\partial g/\partial n$ is

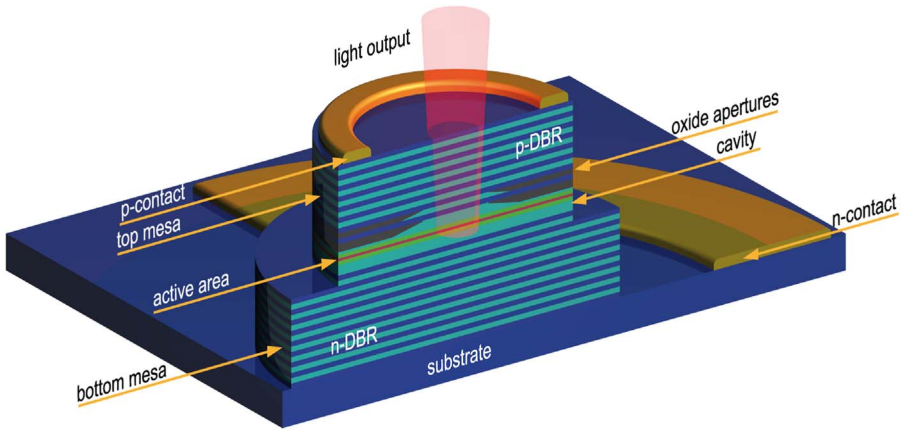

Fig. 1. (Color online) Schematics of a conventionally oxidized VCSEL.[11] © 2014 IEEE.

the differential gain, V_a is the volume of the active region, and χ is the transport factor. From Eq. (3) it is obvious, that in order to obtain a large D-factor (or resonance frequency), strong confinement of the light, large differential gain, and efficient, fast transport of carriers need to be designed.

The damping γ depends linearly on the K-factor,

$$\gamma = Kf_r^2 + \gamma_0, \tag{4}$$

where γ_0 is an off-set and the K-factor is defined as

$$K = 4\pi^2\left(\tau_p + \frac{\varepsilon\chi}{v_g\partial g/\partial n}\right). \tag{5}$$

From Eq. (5) it follows, that the damping γ can be controlled, e.g. by the photon lifetime τ_p. The damping is increasing with current. The intrinsic damping limited bandwidth is given by Eq. (6).

$$f_{3dB,damping} = \frac{2\pi\sqrt{2}}{K}. \tag{6}$$

The measured bandwidth of a VCSEL is usually much smaller than the intrinsic bandwidth, because of thermal and parasitic effects. Reducing these effects to come closer to the intrinsic limits is one of the subjects of this paper.

If the current is increased, the temperature of the device increases due to quantum efficiencies well below 100%. The emission wavelength shifts to larger values, eventually out of resonance with the DBRs. Then a thermally-limited bandwidth is reached. Figure 2 shows a typical thermally induced roll-over of the resonance frequency.[12] In order to realize large thermally-limited bandwidths and to reduce the initial off-set between gain peak and reflectivity minimum, one needs to reduce the self-heating in the VCSEL. Reduction can be realized by lowering the series resistance, the free-carrier absorption in the resonator and by increasing the thermal conductivity.

Controlling thermal effects is still not sufficient to reach the intrinsic bandwidth because of the parasitics, which limit the modulation frequency of the VCSEL. To increase the parasitics limited bandwidth, one needs to lower the oxide capacitance and in particular the series resistance, e.g. by finding alternative solutions for current injection, which is done here.

The design of present high-speed GaAs-based VCSELs has more or less squeezed out the existing potential to

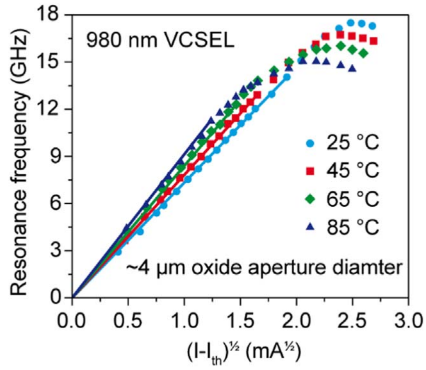

Fig. 2. (Color online) Typical thermally induced roll-over of the resonance frequency of VCSELs.[12] © 2014 IEEE.

optimize intrinsic modulation speed, thermal effects, and parasitics:

- Strained QWs lead to high differential gain.[13–15]
- A short cavity and small oxide apertures lead to a large confinement factor.[16–18]
- Reduced series resistance,[19] high-thermal-conductivity DBRs[20,21] and efficient heat sinks[22,23] are designed to reduce the thermal effects on the bandwidth of VCSELs.
- Series resistance is reduced by using modulation doped interfaces in the DBRs.[24]
- Low dielectric constant insulating materials reduce the pad capacitance,[25,26] and multiple deep oxidation layers or proton implantation bring down the mesa capacitance.[27–29] Figure 3 shows a simplified equivalent circuit model taken from Ref. 30.
- Finally, data rate dependent optimization of output power and energy efficiency were demonstrated by adapting the

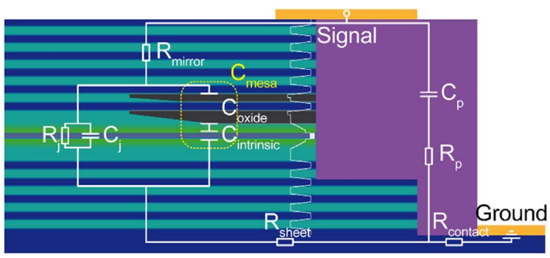

Fig. 3. (Color online) Cross-sectional schematics of the epitaxial structure including parasitic capacitances and resistances.[30] © 2015 IEEE.

reflectivity of the top DBR and thus the photon lifetime.[9,31,32]

3. Performance of high-speed VCSELs

3.1. Modulation bandwidth

At a wavelength of 850 nm, the group at Chalmers University of Technology (CUT) realized 30 GHz bandwidth VCSEL by using the five strained InGaAs QWs, six deep oxide apertures, graded interfaces and modulation doped DBRs. The photon lifetime was varied by shallow surface etching.[33]The Holonyak group at University of Illinois Urbana-Champaign (UIUC) used narrow apertures to enhance the bandwidth of oxide-confined VCSEL to 30 GHz.[34] Finisar also demonstrated ~30 GHz bandwidth VCSELs in 2018.[35] At a wavelength of 940 nm, National Central University (NCU) demonstrated similar bandwidths by using Zn-diffusion and oxide-relief methods.[36] At 980 nm, the group of Lott at Technische Universität Berlin realized 35 GHz bandwidth "simplicity VCSELs" for a 3 μm oxide aperture and low reflectance of the output coupling mirror (below 0.99) consisting of 14.5 mirror pairs.[37] No large signal modulation results were presented. At the longer wavelength of 1060 nm, the group at CUT achieved 23 GHz bandwidth single mode VCSELs by using strain-compensated InGaAs/GaAsP QWs, $\lambda/2$ cavity length, DBRs with step-graded interfaces, optimized modulation doped DBRs, and multiple oxide apertures.[38]

In order to further extend the bandwidth of VCSELs, the resonator of the VCSEL can be coupled to a neighboring resonator to use photon-photon resonances (PPRs) at frequencies larger than the carrier-photon resonance frequency. Koyama's group at Tokyo Institute of Technology demonstrated close to 30 GHz modulation bandwidth of VCSELs using PPR created by a bow-tie shaped transverse coupled cavity.[39–41] Choquette's group at the UIUC realized 37 GHz modulation bandwidth using PPR created by laterally coupled photonic crystal cavities.[42–44] Most recently, 45 GHz modulation bandwidth of VCSEL was realized by using six feedback coupled cavities.[45] The challenge for such complex arrangements is to maintain under practical circumstances the critical feedback and coupling conditions when current and temperature varies. For parts of this work no data transmission experiments were presented.

3.2. Data transmission for short distance interconnects

Based on the VCSELs with large cut-off frequency, enormous increase of data rates for short distance (less than 300 m) has been reported under both NRZ-OOK (PAM-2) modulation and PAM-4 modulation.

At 850 nm, in 2011, the Bimberg group at TU Berlin realized 17 Gbit s^{-1} and 25 Gbit s^{-1} NRZ-OOK data transmission across 100 m and 500 m OM 3 MMF with a then record low energy consumption of 81 fJ bit^{-1}.[46] In 2013, Westbergh et al. used 850 nm VCSELs and realized NRZ-OOK data transmission at 44 Gbit s^{-1} across 50 m OM4 MMF.[47] By varying the photon lifetime of their VCSELs, they realized (back-to-back) BTB 57 Gbit s^{-1} under NRZ-OOK modulation.[48] Even larger link capacity based on 850 nm VCSEL is available by using equalization. Kuchta et al. used transmitter and receiver equalization to demonstrate NRZ-OOK transmission at 64 Gbit s^{-1} across 57 m MMF.[49] Then they realized a record of 71 Gbit s^{-1} NRZ-OOK transmission across 7 m MMF using BiCMOS-driver ICs with feed-forward equalization (FFE).[7] In 2020, Chorchos et al. presented 80 Gbit s^{-1} (or 72 Gbit s^{-1}) NRZ-OOK data transmission through 2 m MMF (or 50 m MMF) by FFE[50] at 850 nm. In none of the papers[45–48] data on the energy efficiency (fJ bit^{-1}) were given. It can be assumed that attempts like FFE to increase the data rate increases additionally energy consumption.

Work on high bit rate NRZ-OOK data transmission in MMF links was also carried out for 980 nm, 1060 nm and 1100 nm VCSELs.[25,31,38,51,52] Compared to 850 nm high-speed VCSEL, devices emitting at longer wavelengths benefit from larger temperature insensitivity of the quantum efficiency due to reduced carrier spill-out of the well, lower chromatic dispersion and lower transmission loss in MMF. At 980 nm, the TU Berlin group demonstrated 46 Gbit s^{-1} NRZ-OOK data transmission at 85 °C.[52] By optimizing the photon lifetime of 980 nm VCSEL, Larisch et al. increased the data rate to 50 + Gbit s^{-1} at 85 °C,[31] a number still limited by the set-up. Simpanen and co-workers realized 50 Gbit s^{-1} NRZ-OOK data transmission using 1060 nm VCSEL with 100 fJ bit^{-1} energy dissipation.[38] Table I compares these results.

Under PAM-4 modulation, much of the recent research work was carried out at 850 nm.[53,54] Without any equalization or digital signal processing, in 2011 Szczerba et al. realized 30 Gbit s^{-1} (or 25 Gbit s^{-1}) PAM-4 data transmission across 200 m (or 300 m) MMF.[55] Then, they increased the date rate to 60 Gbit s^{-1} (or 50 Gbit s^{-1}) across 2 m (or 50 m) MMF[56] and demonstrated a BTB capacity of 94 Gbit s^{-1} with equalization and forward error correction (FEC).[57] In 2015, Zuo et al. at from Huawei demonstrated 112 Gbit

Table I. Selected values for bit rates of VCSELs and short fiber lengths under NRZ-OOK modulation.

Group	Wavelength (nm)	Bit rate (Gbit s^{-1})	Fiber length (m)	Year	References
TU Berlin-VIS	850	25	100	2011	46
CUT	850	47 (44)	BTB (50)	2013	47
CUT	850	57 (55)	BTB (50)	2013	48
IBM-CUT	850	64	57	2014	49
IBM-CUT	850	71	7	2015	7
WUT-VIS	850	80 (72)	2 (50)	2020	50
UCSB	980	35	\	2007	25
TU Berlin	980	46	\	2016	52
TU Berlin	980	52	\	2016	31
CUT-HPE	1060	50	\	2017	38
NEC	1100	25	\	2009	51

s^{-1} PAM-4 transmission across 200 m MMF.[58] With equalization and FEC, the PAM-4 transmission was increased to 155 Gbit s^{-1} (or 100 Gbit s^{-1}) across 100 m (or 300 m) in 2016,[59] and with a Volterra nonlinear equalizer, partial response signaling, and a noise cancellation module, it was further increased to 200 Gbit s^{-1} across 100 m MMF[60] by the same group. In 2017, Lavrencik and co-workers employed equalization and pulse shaping to increase the data rate to 110 Gbit s^{-1} for PAM-4 transmission across 100 m wideband MMF.[61] With discrete multitone, equalization, and FEC, Kottke et al. realized 120 Gbit s^{-1} PAM-4 transmission across 300 m MMF.[62] In 2019/20, Lavrencik et al. transmitted 168/100 Gbit s^{-1} across 50/100 m OM5 MMF using PAM-4.[63] Using complex 1.3 μm wafer-fusion VCSELs Wolf et al. achieved 2017 a bit rate close to 40 Gb s^{-1} by PAM-4.[64] Table II compares these results.

3.3. Data transmission at larger distances

Given the rapidly increasing size of data centers, transmission at distances up to 2000 m is desirable. Single mode VCSELs (SM-VCSELs) are preferred, because of the reduced impact of fiber chromatic dispersion and the ease of dense wavelength multiplexing for wavelength differences of 5 nm like for edge emitting laser based MANs at 1.3 μm.

In 2014, CUT demonstrated 20 Gbit s^{-1} and 25 Gbit s^{-1} NRZ-OOK data transmission through 2000 m and 1300 m OM4 fibers, respectively, using 850 nm SM-VCSEL,[65] without FEC or equalization. In 2016, by using equalization and FEC, Warsaw University of Technology (WUT) and VI Systems achieved 54 Gbit s^{-1} data transmission, again using 850 nm SM-VCSELs across 2200 m OM4 fiber.[8] In 2018, the same two groups used 850 nm/910 nm SM-VCSEL and realized 25 Gbit s^{-1} NRZ-OOK data transmission across 2600 m/2400 m OM5 fibers using FEC.[66]

Under PAM-4 modulation, Finisar reported 50 Gbit s^{-1} across 2300 m OM4 fiber using 850 nm VCSEL with equalization and FEC.[67] Liu and co-workers demonstrated 64 Gbit s^{-1} PAM-4 data transmission over 2000 m OM4 fibers using 850 nm VCSEL and a nonlinear equalizer.[68] HPE realized 50 Gbit s^{-1} PAM-4 data transmission through 2000 m SMF using a 1060 nm SM-VCSEL and FEC.[69] Again, data on the energy efficiency (fJ bit^{-1}) were almost never given the results mentioned above are just indicative of the progress achieved in the last years and by far not complete. Table III compares these results.

4. Adapt photon lifetime of VCSELs to data rate

Most recently the topic of energy consumption as a function of the bit rate emerged as decisive for future device and module design. The studies summarized above show, that the bit rates of optical links can be increased by using higher order modulation formats like PAM-4, and drivers with FEC and equalization. However, the energy cost per bit for data transmission at larger bit rates needs to be compared with that of data transmission at lower bit rates using wavelength multiplexing at the smaller rates, still achieving the same transmission capacity. By depositing SiN on the surface of the top DBR the photon lifetime and the damping of VCSELs can be tuned[31] and the output power (Fig. 4) and the cut-off frequency of the VCSEL can be increased. Smaller oxide-aperture VCSELs usually have larger cut-off frequencies and are more energy efficient, and can meet the power-budge requirements of the optical link. Using this method, error free bit rates of 52 Gbit s^{-1} NRZ-OOK data transmission was achieved with comparatively low energy consumption.[31]

Coarse wavelength division multiplexing, being standardized (e.g. Ethernet 802.3bs and CEI-56G), is helpful for the implementation of strategies for optimizing the energy to data ratio (EDR) of an optical link. The number of VCSELs in a WDM system does not only increase the bandwidth of the link. Choosing of the number of VCSELs presents a new degree of freedom to optimize the energy consumption for a target bit rate.

Figure 5 presents the experimental results for the EDR as a function of bite rate (BR) for a long photon lifetime (blue curve) and a short photon lifetime (the red curve), achieved by evaporation of SiN on the top mirror. The spectral efficiency has also been determined experimentally based on large signal measurement results marked with (a) and (c) for both photon lifetimes.[31,70] There is a crossover between the two curves in Fig. 5. They can be separated into two areas by the grey dashed line going through the crossover. We add the explanation in the revised manuscript (page 8, the third paragraph).

'The bit rate dependent energy consumption of a VCSEL is a function of the damping, controlled by the photon lifetime (see Ref. 9). The energy consumption of VCSELs with short photon lifetime is less than that of those with a long photon lifetime for the same BR beyond a certain bit rate, given by the grey line in Fig. 5. The bit rate dependent energy consumption of a VCSEL is a function of the damping, controlled by the photon lifetime (see Ref. 9). The energy consumption of VCSELs with short photon lifetime is less than that of those with a long photon lifetime for the same BR beyond a certain bit rate, given by the grey

Table II. Selected values for bit rates of VCSELs and short fiber lengths under PAM-4 modulation.

Group	Wavelength (nm)	Bit rate (Gbit s^{-1})	Fiber length (m)	Year	References
CUT	850	30 (25)	200 (300)	2011	53
CUT	850	60	BTB	2013	54
CUT	850	94	BTB	2016	55
Huawei	850	112	200	2015	56
Huawei-Keysight	850	112	100	2016	57
Huawei-VI-Systems	850	155 (100)	100 (300)	2016	58
Huawei	850	200	100	2020	59
WUT-VI Systems	850	108	100	2016	60
Georgia Tech	850	110	100	2017	61
Fraunhofer-TU Berlin-VI Systems	850	120	300	2017	62
Georgia Tech-VI Systems-WUT	850	168	50	2020	63
Georgia Tech-VI-Systems-HPE	1060	100	100	2019	64

Table III. Selected values for bit rates of SM-VCSELs and long fiber lengths.

Group	Wavelength (nm)	Bit rate (Gbit s^{-1})	Modulation	Fiber length (m)	Year	References
CUT	SM 850	20 25	NRZ-OOK	SMF 2000 SMF 1300	2014	65
WUT- VI system	SM 850	54	NRZ-OOK	SMF 2200	2016	8
WUT- VI system	SM 850 SM 910	25	NRZ-OOK	MMF 2600 MMF 2400	2018	66
Finisar	MM 850	50	PAM-4	MMF 2300	2018	67
NCTU- NCU-NSYU	FW 850	64	PAM-4	MMF 2000	2017	68
HPE	SM 1060	50	PAM-4	SMF 2000	2017	69

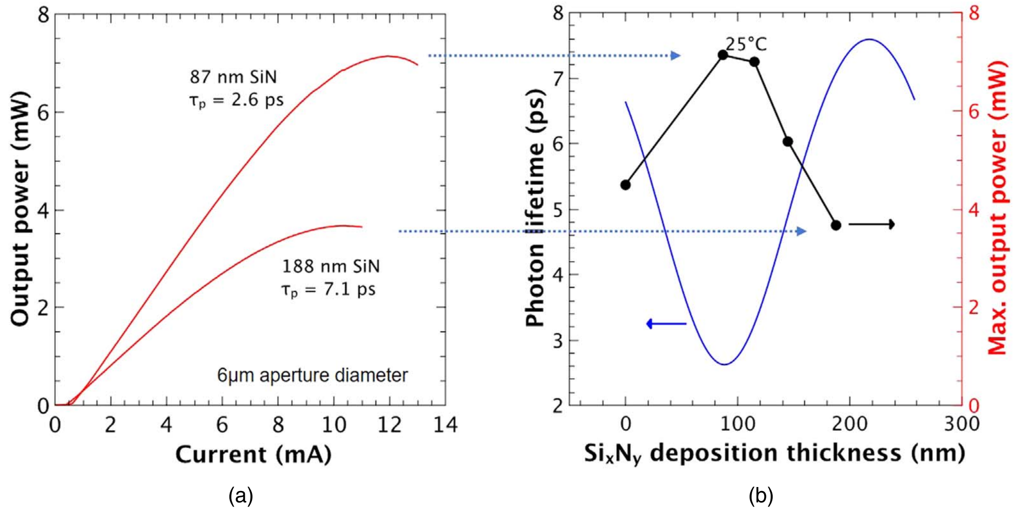

Fig. 4. (Color online) (a) Output power as a function of current of a 6 μm oxide aperture diameter VCSELs with different thicknesses of SiN and photon lifetime. (b) Photon lifetime and max. output power of the VCSEL as a function of thickness of SiN.[31] © 2016 IEEE.

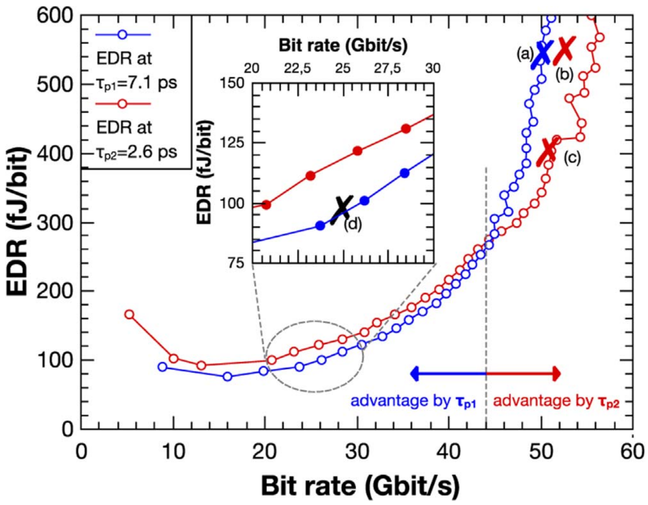

Fig. 5. (Color online) EDR and BR values from small signal measurements, for a long photon lifetime (blue) and a short photon lifetime (red). The spectral efficiency of $M = 2.1$ bit was found experimentally by the large signal measurement results marked with (a) and (c) for both photon lifetimes. The data points marked with (a), (b), and (c) as well as the curves are achieved with the identical device. Datapoint (d) was measured with a different similar aperture device.[71] © 2020 OSA.

line in Fig. 5. Therefore, at larger bit rates (>44 Gbit s^{-1}), it is advantageous to use VCSELs with a short photon lifetime, whereas at medium or small bit rates, it is advantageous to use devices with a long photon lifetime, both from energy-consumption point of view. At least 25% reduction of EDR is achieved for both 50 Gbit s^{-1} and 25 Gbit s^{-1} data rates by choosing optimum photon lifetimes of the VCSELs.

WDM for 200+ Gbit s^{-1} data transmission was demonstrated by using 850 nm, 880 nm, 910 nm and 940 nm VCSELs (Fig. 6).[71] 200 Gbit s^{-1} data transmission can also be realized by using instead eight VCSELs each at a bit rate of only 25 Gbit s^{-1}. The best EDR at 50 Gbit s^{-1} is 400 fJ bit^{-1} by using VCSELs with a short photon lifetime, while the EDR at 25 Gbit s^{-1} is less than 100 fJ bit^{-1} by using VCSELs with a long photon lifetime. Therefore, for the same 200 Gbit s^{-1} optical link, over 50% energy reduction is achieved by adaptive photon lifetime tuning and WDM. In addition, the lower current density at the operating conditions for 25 Gbit s^{-1} leads to less heat and reduces the risk of device failure.

The noise of the VCSEL dominates the noise of the whole link and determines the spectral efficiency M.[72] By increasing the photon lifetime, the K-factor will be increased, and thus the damping is increased, leading to a reduction of the noise.[73,74] Therefore, VCSELs with long photon lifetime are beneficial for increasing the spectral efficiency M, and are more suitable for higher order modulation formats to increase the data rate.

5. Novel processing approach for aperture formation improving heat conduction and reducing series resistance

Figure 2 is an excellent example demonstrating the influence of heat, leading to thermal roll-over. The epitaxial structure was designed such that there is an off-set between the room temperature peak of emission and the maximum transmission of the DBRs. The emission peak at RT is positioned at comparatively shorter wavelength in order to have a flat response with increasing temperature. Thus, the initial slope of the resonance frequency curves is largest for temperatures around 85 °C. It bends over, however, at lower currents than

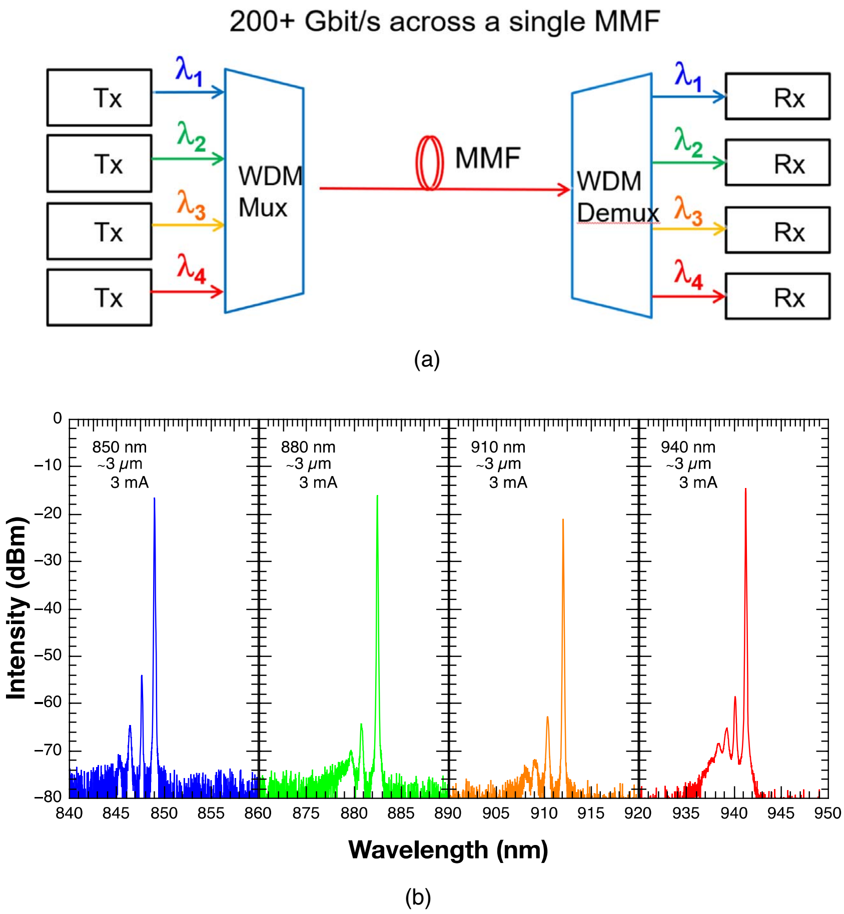

Fig. 6. (Color online) (a) Experimental set-up of the 200 Gbit s^{-1} optical link across a single MMF by WDM. (b) Emission spectra of single mode emitting lasers with 3 μm oxide aperture diameter at the wavelengths 850 nm, 880 nm, 910 nm, and 940 nm.[9] © 2019 IEEE.

those of the curves at lower temperatures and has a lower maximum frequency. All the curves show thermal roll-over, but each of them at a different current. The largest frequency at roll-over is observed for the RT experiments. This systematics is readily understood keeping in mind, that the temperature inside the active area on top of the experimentally set temperature increases with increasing current as a consequence of a slope quantum efficiency below 100%. The actual active area temperature depends to on the heat dissipation of the structure.

We developed a completely novel approach to oxidize the apertures.[75] A number of holes is etched in the epitaxial structure in a symmetric square, hexagonal,… or an asymmetric arrangement to a depth just the below the last AlAs layer to be oxidized, as shown in Fig. 7. For an aperture ending on top of the active area one would etch to the active area. The aperture(s) is/are oxidized from these holes. Figure 8 shows an SEM cross-section after oxidation for a square arrangement. Thus, almost any geometry for one aperture or an array of multiple apertures next to each other is possible. Once the oxidation is terminated the side walls of the holes can be

a. either covered with an insulator and then filled with metal or

b. directly filled with metal.

In both cases heat dissipation is expected to be largely improved, since transport of phonons through the top mirror, with its p-doping and many phonon reflecting interfaces is circumvented. Case b. additionally connects the active area/s directly with the p-side contact and is expected to reduce the series resistance considerably. Classical VCSELs show a large series resistance of several hundred Ohm for narrow apertures, being prerequisite for single mode emission. Typical drivers with low impedance are suddenly matched to the laser, presenting a break-through for the complete system. Novel high-speed CMOS driver circuits showing much lower energy consumption of the module, can be matched and both together will present an important step towards green photonics for a sustainable future.

Another very important feature of our novel design presents the possibility to drive the devices at larger currents and thus achieve much larger 3 dB cut-off frequencies with little overshoot, flat response There will be no need to reduce the number of mirrors to achieve these advantages, which will leed to low noise and ease higher order modulation schemes, like PAM-4, etc.

The novel VCSEL fabrication is compatible to present ones and can be readily incorporated into any existing processing infrastructure.

6. Moving from single aperture devices to multi-aperture ones

In Chap. 3.3, we discussed, that high power SM-VCSELs are essential for long distance data transmission, enabling dense wavelength multiplexing based on existing fiber designs. Using narrow oxide-apertures is the only way to achieve single mode emission and thus large cut-off frequencies. Presently narrow oxide-aperture lasers show small output

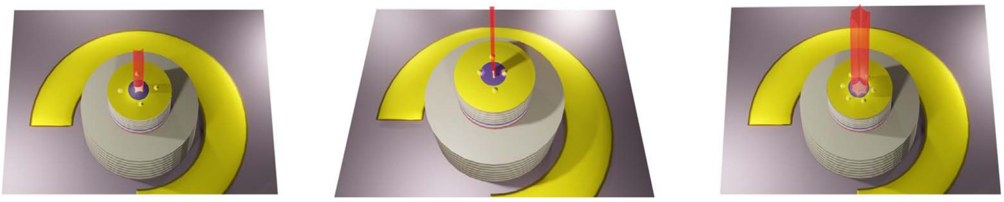

(a) (b) (c)

Fig. 7. (Color online) Schematic of the novel design VCSEL with holes in (a) symmetric square, (b) asymmetric square and (c) six-fold arrangement.

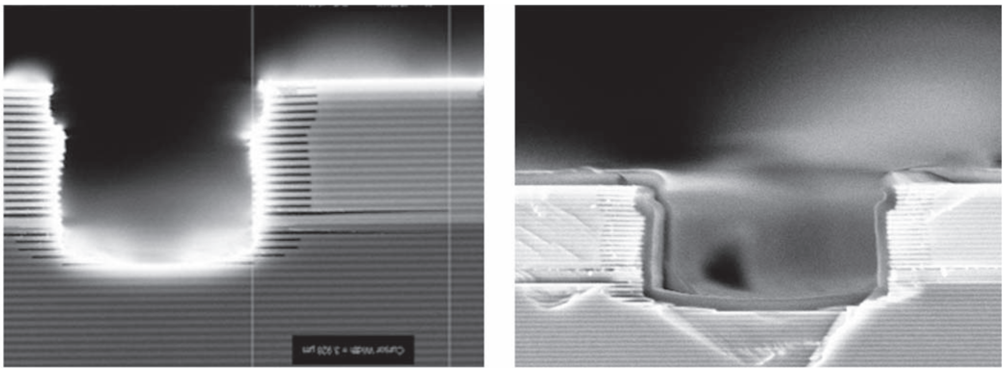

(a) (b)

Fig. 8. (Color online) (a) SEM of the cross-section of one hole after oxidation. (b) SEM of the cross-section of one hole after deposition of an insulating layer and metal at its circumference.

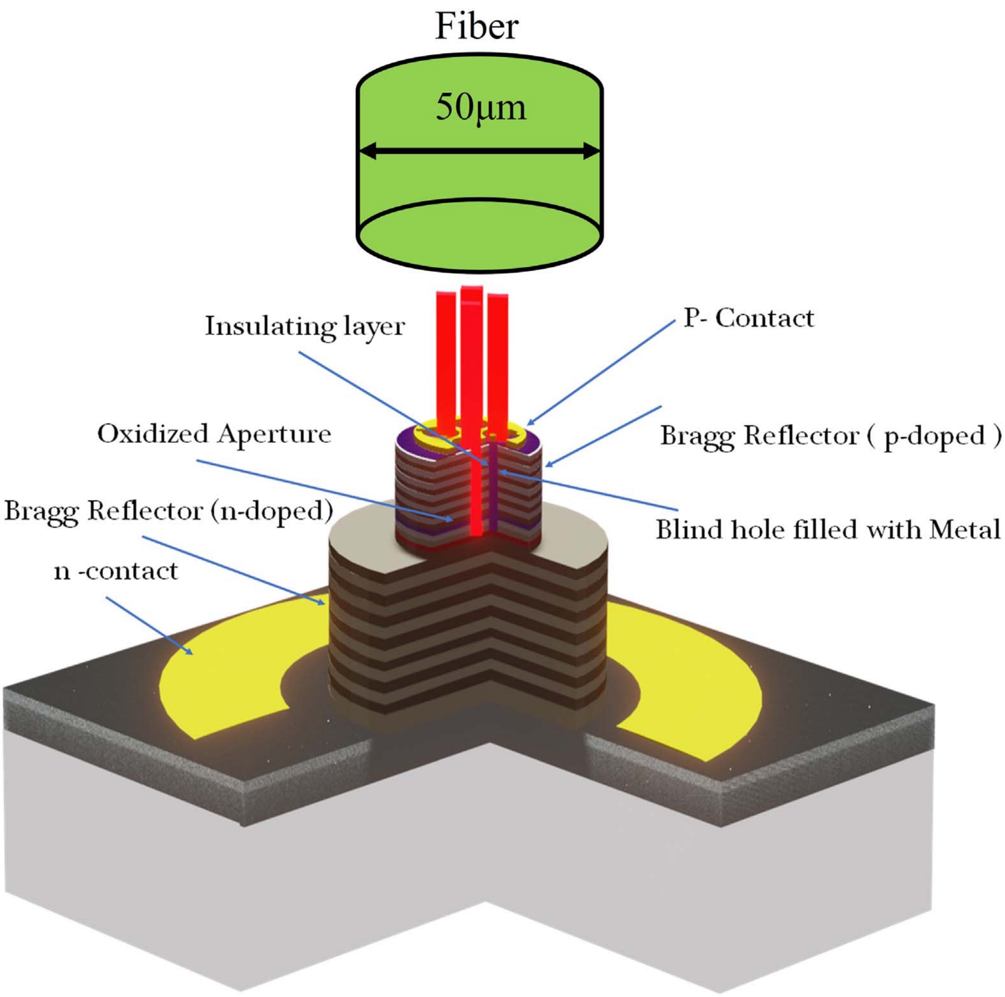

Fig. 9. (Color online) The schematic of a MAVs with four apertures. The light emission from all apertures can be easily collected by a 50 μm fiber.

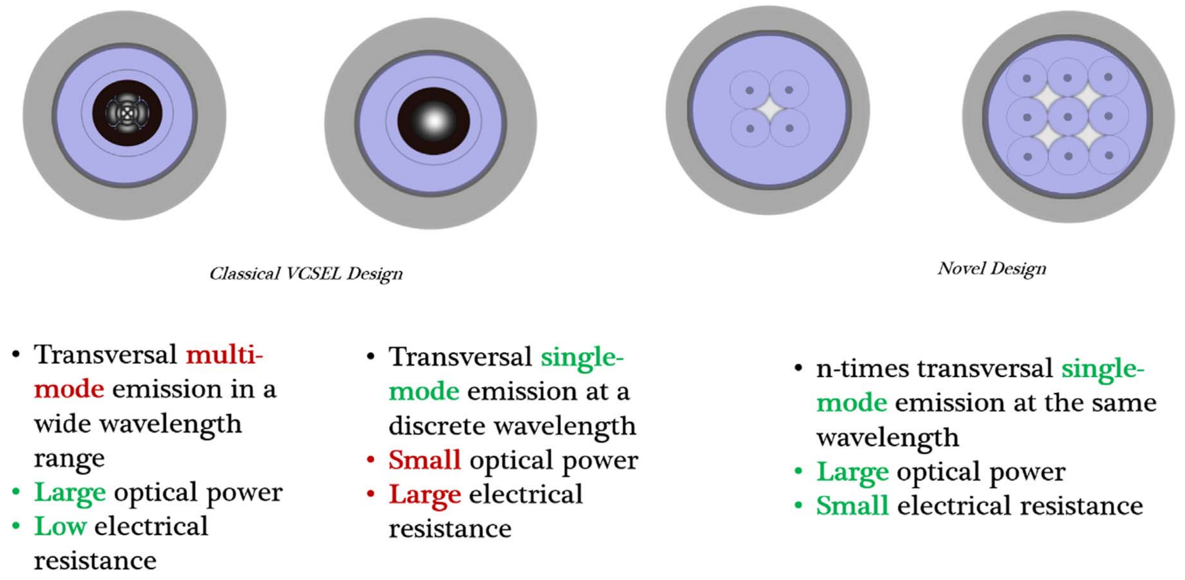

Fig. 10. (Color online) Comparing properties of novel and classical VCSEL designs.

power and a larger series resistance of VCSEL, as compared to large aperture ones, being multi-mode. Section 5 presented a novel design concept for fabricating single mode high power lasers. This concept can be easily extended to a multi-aperture one.[75] The schematics of our novel Multi-Aperture VCSELs, MAVs, is shown in Fig. 9[76] together with its connection to an optical fiber. Additional enormous performance advantages, like temperature roll-over at larger currents, larger output power, and larger cut-off frequency (the decisive parameter determining the bit rate), are expected.

The novel multi-aperture design with "*n*" number of apertures can produce "*n*" times single mode power at the same discrete wavelength, showing still small series resistance, lower operating temperature of the active area, larger cut-off frequency, compared to a standard VCSEL. Figure 10 shows a comparison. One mesa containing multiple emitters will still be matched to a 50 μm diameter fiber.

Further future design variants will enable orthogonal polarization multiplexing.[77]

7. Summary and outlook

In this review, a survey is given of the success and limits of the present design of high-speed VCSELs and its implications for power budget and performance of optical links Photon lifetime management is emphasized as an approach to make classical VCSEL design adaptive to system demands Two completely novel design approaches for single and multi-aperture VCSELs based on GaAs technology are introduced. Both approaches are based on oxide aperture formation from variable geometry holes etched in the wafer and filled with metal after etching. Large improvement of thermal properties, the output power, the cut-off frequency and the energy consumption of devices in particular with single mode emissions are expected. Several apertures can be combined in one device, additionally increasing single mode output power or allowing polarization multiplexing. Details of the processing are demonstrated.

The new design concepts can be also used for fabricating QD-based VCSELs in the infrared window 1.23–1.31 μm, particularly important for automotive applications like LIDAR. QD-VCSELS based on multiple hole aperture formation are expected to show large energy efficiency, in parallel to the record low threshold current density of QD-based devices shown in the past[78–80] for edge emitting QD-lasers. The huge advantage of this IR wavelength of window is, that inexpensive and large area GaAs technology can be extended to new fields of applications. QD-VCSELs emitting in the 1.23–1.31 μm range are suggested by us to be advantageous for automotive applications, where the maximum allowed power is orders of magnitude larger than for the present- lasers emitting at 905 nm, dominating the market.

Acknowledgments

The authors would like to thank Gunter Larisch and Julian Lindner for their cooperation. The authors appreciate the support of the National Key R&D Program of China (2021YFB2801000 and 2018YFB2201000), National Natural Science Foundation of China (61774156, 62174159 and 62061136010), CAS Youth Innovation Promotion Association (2018249), Sino-German Center for Research Promotion (joint Mobility Program of DFG and NNSFC M0386), Natural Science Foundation of Jilin Province (20210402055GH).

1) Global Internet Growth and Trends (Source: Cisco VNI Global IP Traffic Forecast, 2017–2022), [https://cisco.com/c/en/us/solutions/collateral/executive-perspectives/annual-internet-report/white-paper-c11-741490.pdf].
2) D Bimberg, In 2021 26th Microoptics Conf. (MOC2021), p. PL2-2.
3) D. Mahgerefteh, C. Thompson, C. Cole, G. Denoyer, T. Nguyen, I. Lyubomirsky, C. Kocot, and J. Tatum, J. Lightwave Technol. **34**, 233 (2016).
4) J. A. Tatum et al., J. Lightwave Technol. **33**, 727 (2015).
5) P. Moser, J. A. Lott, G. Larisch, and D. Bimberg, J. Lightwave Technol. **33**, 825 (2015).
6) K. Szczerba, P. Westbergh, M. Karlsson, P. A. Andrekson, and A. Larsson, J. Lightwave Technol. **33**, 1395 (2015).

7) D. M. Kuchta, A. V. Rylyakov, F. E. Doany, C. L. Schow, J. E. Proesel, C. W. Baks, P. Westbergh, J. S. Gustavsson, and A. Larsson, IEEE Photonics Technol. Lett. **27**, 577 (2015).
8) G. Stepniak, A. Lewandowski, J. R. Kropp, N. N. Ledentsov, V. A. Shchukin, N. Ledentsov Jr., G. Schaefer, M. Agustin, and J. P. Turkiewicz, Electron. Lett. **52**, 633 (2016).
9) G. Larisch, R. Rosales, and D. Bimberg, IEEE J. Sel. Top. Quantum Electron. **25**, 1701105 (2019).
10) [Available: https://ethernetalliance.org/the-2018-ethernet-roadmap/].
11) H. Li, P. Wolf, P. Moser, G. Larisch, J. Lott, and D. Bimberg, SPIE Newsroom **1**, 1 (2014).
12) H. Li, P. Wolf, P. Moser, G. Larisch, A. Mutig, J. A. Lott, and D. H. Bimberg, IEEE J. Quantum Electron. **50**, 613 (2014).
13) S. B. Healy, E. P. O. Reilly, J. S. Gustavsson, P. Westbergh, Å Haglund, A. Larsson, and A. Joel, IEEE J. Quantum Electron. **46**, 506 (2010).
14) P. Westbergh, J. S. Gustavsson, Å Haglund, M. Skold, A. Joel, and A. Larsson, IEEE J. Sel. Top. Quantum Electron. **15**, 694 (2009).
15) I. Suemune, IEEE J. Quantum Electron. **27**, 1149 (1991).
16) P. Moser, P. Wolf, A. Mutig, G. Larisch, W. Unrau, W. Hofmann, and D. Bimberg, Appl. Phys. Lett. **100**, 081103 (2012).
17) H. W. Then, C. H. Wu, M. Feng, and N. H. Jr, Appl. Phys. Lett. **96**, 131107 (2010).
18) W. Hofmann, P. Moser, P. Wolf, A. Mutig, M. Kroh, and D. Bimberg, Optical Fiber Communication Conf./National Fiber Optic Engineers Conf. 2011 (Optical Society of America, Los Angeles, California, 2011), p. PDPC5.
19) P. Zhou et al., IEEE Photonics Technol. Lett. **3**, 591 (1991).
20) W. Nakwaski and M. Osiński, in *Progress in Optics*, ed. E. Wolf, (Elsevier, Amsterdam, 1998), p. 165.
21) M. A. Afromowitz, Appl. Phys. Lett. **44**, 1292 (1973).
22) A. N. Al-Omari, M. S. Alias, A. Ababneh, and K. L. Lear, J. Phys. D: Appl. Phys. **45**, 505101 (2012).
23) R. Pu, C. W. Wilmsen, K. M. Geib, and K. D. Choquette, IEEE Photonics Technol. Lett. **11**, 1554 (1999).
24) E. F. Schubert, L. W. Tu, G. J. Zydzik, R. F. Kopf, A. Benvenuti, and M. R. Pinto, Appl. Phys. Lett. **60**, 466 (1992).
25) Y.-C. Chang, C. S. Wang, and L. A. Coldren, Electron. Lett. **43**, 1022 (2007).
26) A. N. A.-. Omari and K. L. Lear, IEEE Photonics Technol. Lett. **16**, 969 (2004).
27) N. Suzuki, H. Hatakeyama, K. Fukatsu, T. Anan, K. Yashiki, and M. Tsuji, Electron. Lett. **42**, 975 (2006).
28) Y.-C. Chang, C. S. Wang, L. A. Johansson, and L. A. Coldren, Electron. Lett. **42**, 1281 (2006).
29) M. Azuchi, N. Jikutani, M. Arai, T. Kondo, and F. Koyama, "Multioxide layer vertical-cavity surface-emitting lasers with improved modulation bandwidth," 5th Pacific Rim Conf. on Lasers and Electro-Optics, Vol. 1, p. 163, 2004.
30) H. Li, J. A. Lott, P. Wolf, P. Moser, G. Larisch, and D. Bimberg, IEEE Photonics Technol. Lett. **27**, 832 (2015).
31) G. Larisch, P. Moser, J. A. Lott, and D. Bimberg, IEEE Photonics Technol. Lett. **28**, 2327 (2016).
32) P. Westbergh, J. S. Gustavsson, B. Kögel, Å Haglund, and A. Larsson, IEEE J. Sel. Top. Quantum Electron. **17**, 1603 (2011).
33) A. Larsson, M. Geen, J. S. Gustavsson, E. Haglund, A. Joel, P. Westbergh, and E. Haglund, Electron. Lett. **51**, 1096 (2015).
34) M. Feng, C. Wu, and N. Holonyak, IEEE J. Quantum Electron. **54**, 2400115 (2018).
35) J. A. Tatum, G. D. Landry, D. Gazula, J. K. Wade, and P. Westbergh, Optical Fiber Communication Conf. (Optical Society of America, San Diego, California, 2018), p. M3F.6.
36) C. L. Cheng, N. Ledentsov, Z. Khan, J. L. Yen, N. N. Ledentsov, and J. W. Shi, IEEE J. Sel. Top. Quantum Electron. **25**, 1700507 (2019).
37) N. Haghighi, G. Larisch, R. Rosales, M. Zorn, and J. A. Lott, In 2018 IEEE Int. Semiconductor Laser Conf. (ISLC2018), p. 1.
38) E. Simpanen, J. S. Gustavsson, E. Haglund, E. P. Haglund, A. Larsson, W. V. Sorin, S. Mathai, and M. R. Tan, Electron. Lett. **53**, 869 (2017).
39) M. Ahmed, A. Bakry, M. S. Alghamdi, H. Dalir, and F. Koyama, Opt. Express **23**, 15365 (2015).
40) H. Dalir and F. Koyama, Appl. Phys. Express **7**, 022102 (2014).
41) H. Dalir and F. Koyama, Appl. Phys. Lett. **103**, 091109 (2013).
42) H. Dave, Z. Gao, S. T. M. Fryslie, B. J. Thompson, and K. D. Choquette, IEEE J. Sel. Top. Quantum Electron. **25**, 1700208 (2019).
43) S. T. M. Fryslie et al., IEEE J. Sel. Top. Quantum Electron. **23**, 1700409 (2017).
44) S. T. M. Fryslie, M. P. T. Siriani, D. F. Siriani, M. T. Johnson, and K. D. Choquette, IEEE Photonics Technol. Lett. **27**, 415 (2015).
45) E. Heidari, H. Dalir, M. Ahmed, V. J. Sorger, and R. T. Chen, Nanophotonics **9**, 4743 (2020).
46) P. Moser, W. Hofmann, P. Wolf, J. A. Lott, G. Larisch, A. Payusov, N. N. Ledentsov, and D. Bimberg, Appl. Phys. Lett. **98**, 231106 (2011).
47) P. Westbergh, R. Safaisini, E. Haglund, J. S. Gustavsson, A. Larsson, M. Geen, R. Lawrence, and A. Joel, IEEE Photonics Technol. Lett. **25**, 768 (2013).
48) P. Westbergh, E. Haglund, E. Haglund, R. Safaisini, J. S. Gustavsson, and A. Larsson, Electron. Lett. **49**, 1021 (2013).
49) D. M. Kuchta, A. V. Rylyakov, C. L. Schow, J. E. Proesel, C. Baks, P. Westbergh, J. S. Gustavsson, and A. Larsson, In Optical Fiber Communication Conf. (Optical Society of America, San Francisco, California, 2014), p. Th3C.2.
50) L. Chorchos, N. Ledentsov, J. R. Kropp, V. A. Shchukin, V. P. Kalosha, A. Lewandowski, J. P. Turkiewicz, and N. N. Ledentsov, J. Lightwave Technol. **38**, 1747 (2020).
51) H. Hatakeyama, T. Akagawa, K. Fukatsu, N. Suzuki, K. Tokutome, K. Yashiki, T. Anan, and M. Tsuji, Electron. Lett. **45**, 45 (2009).
52) P. Moser, J. A. Lott, P. Wolf, G. Larisch, H. Li, and D. Bimberg, Electron. Lett. **50**, 1369 (2014).
53) W. C. Lo, W. L. Wu, C. H. Cheng, H. Y. Wang, C. T. Tsai, C. H. Wu, and G. R. Lin, IEEE J. Sel. Top. Quantum Electron. **28**, 1500409 (2022).
54) M. J. Li et al., J. Lightwave Technol. **39**, 868 (2021).
55) K. Szczerba, P. Westbergh, J. Karout, J. Gustavsson, Å. Haglund, M. Karlsson, P. Andrekson, E. Agrell, and A. Larsson, Opt. Express **19**, B203 (2011).
56) K. Szczerba, P. Westbergh, M. Karlsson, P. A. Andrekson, and A. Larsson, Electron. Lett. **49**, 953 (2013).
57) K. Szczerba, T. Lengyel, M. Karlsson, P. A. Andrekson, and A. Larsson, IEEE Photonics Technol. Lett. **28**, 2519 (2016).
58) T. Zuo, L. Zhang, E. Zhou, G. N. Liu, and X. Xu, 2015 European Conf. on Optical Communication (ECOC2015), p. 1.
59) T. Zuo, L. Zhang, J. Zhou, Q. Zhang, E. Zhou, and G. N. Liu, ECOC 2016; 42nd European Conf. on Optical Communication2016), p. 1.
60) T. Zuo, T. Zhang, S. Zhang, and L. Liu, Asia Communications and Photonics Conf./Int. Conf. on Information Photonics and Optical Communications 2020 (ACP/IPOC), (Optical Society of America, Beijing, 2020), p. S3H.2.
61) J. Lavrencik, S. Varughese, J. S. Gustavsson, E. Haglund, A. Larsson, and S. E. Ralph, In 2017 European Conf. on Optical Communication (ECOC2017), p. 1.
62) C. Kottke, C. Caspar, V. Jungnickel, R. Freund, M. Agustin, and N. N. Ledentsov, In 2017 Optical Fiber Communications Conf. and Exhibition (OFC2017), p. 1.
63) J. Lavrencik et al., In Optical Fiber Communication Conf. (OFC) 2019 (Optical Society of America, San Diego, California, 2019), p. M1F.3.
64) P. Wolf, H. Li, A. Caliman, A. Mereuta, V. Iakovlev, A. Sirbu, E. Kapon, and D. Bimberg, ACS Photonics **4**, 2018 (2017).
65) R. Safaisini, E. Haglund, P. Westbergh, J. S. Gustavsson, and A. Larsson, Electron. Lett. **50**, 40 (2014).
66) N. Ledentsov Jr., M. Agustin, L. Chorchos, N. N. Ledentsov, and J. P. Turkiewicz, Electron. Lett. **54**, 774 (2018).
67) S. M. R. Motaghiannezam, A. Tatarczak, H. Chen, J. Tatum, and C. Kocot, Optical Fiber Communication Conf. (Optical Society of America, San Diego, California, 2018), p. M1I.3.
68) J.-J. Liu, K.-L. Chi, C.-C. Wei, T.-C. Lin, C.-Y. Chuang, X.-N. Chen, J.-W. Shi, and J. Chen, In Optical Fiber Communication Conf. (Optical Society of America, Los Angeles, California, 2017), p. W3G.5.
69) M. R. T. Tan, B. Wang, W. V. Sorin, S. Mathai, and P. Rosenberg, IEEE Photonics Technol. Lett. **29**, 1128 (2017).
70) D. Bimberg, G. Larisch, H. Li, P. Moser, P. Wolf, and J. A. Lott, Electron. Lett. **50**, 1369 (2014).
71) G. Larisch, S. C. Tian, and D. Bimberg, Opt. Express **28**, 18931 (2020).
72) C. E. Shannon, Proc. IRE **37**, 10 (1949).
73) T. Lengyel, K. Szczerba, E. P. Haglund, P. Westbergh, M. Karlsson, A. Larsson, and P. A. Andrekson, J. Lightwave Technol. **35**, 4203 (2017).
74) E. P. Haglund, P. Westbergh, J. S. Gustavsson, and A. Larsson, J. Lightwave Technol. **33**, 795 (2015).
75) G. Larisch, S. C. Tian, and D. Bimberg, Radiation emitter, EP 20 192 355.4 + US 17/170,834 + CN113594855A.
76) A. Mansoor, S. C. Tian, J. Lindner, G. Larisch, and D. Bimberg, In 2021 27th Int. Semiconductor Laser Conf. (ISLC2021), p. 1.
77) G. Larisch, S. C. Tian, and D. Bimberg, Radiation emitter, EP 20 210 737.1 + US 17/170,709 + CN113140962A.
78) D. Bimberg, N. N. Ledentsov, M. Grundmann, F. Heinrichsdorff, V. M. Ustinov, P. S. Kop'ev, Z. I. Alferov, and J. A. Lott, Solid-State Electron. **42**, 1433 (1998).
79) D. Bimberg, N. N. Ledentsov, and J. A. Lott, MRS Bull. **27**, 531 (2002).
80) D. Bimberg and U. W. Pohl, Mater. Today **14**, 388 (2011).

Si-Cong Tian received his B. Sc. and Ph.D. degree in Physics from Jilin University, China, in 2007 and 2012, respectively. In 2016–2017 he studied in Arkansas University, US, as a visiting scholar. Currently, he is a Professor at Bimberg Chinese–German Center for Green Photonics, Changchun Institute of Optics Fine Mechanics and Physics, Chinese Academy of Sciences, China. His research interest includes vertical-cavity surface-emitting lasers, high-brightness vertical broad-area edge emitting lasers and photonic crystal lasers.

Mansoor Ahamed is pursuing doctoral study, supervised by Professor Bimberg at Bimberg Chinese–German center for Green Photonics, Changchun Institute of Optical, Fine Mechanics and Physics, Chinese Academy of Science, Jilin, China. His research focus is the development of Multi-aperture VCSEL. He received his Master's degree and Bachelor's degree from India.

Gunter Larisch received the Diploma (M.Sc. equivalent) degree in applied physics and the Ph. D. degree in science from the Technische Universität Berlin, Berlin, Germany, in 2011 and 2017, respectively. He continued working as a Postdoctoral Researcher at Technische Universität Berlin, and then joined Bimberg Chinese–German Center for Green Photonics, Chinese Academy of Sciences, Changchun, China.

Dieter Bimberg (LF'16) received the Ph.D. degree from Goethe University, Frankfurt, Germany, in 1971. He held a Principal Scientist position at the Max Planck Institute for Solid State Research, Grenoble, France, until 1979. After serving as a Professor of Electrical Engineering with the Technical University of Aachen, Aachen, Germany, he assumed the Chair of Applied Physics at the Technical University of Berlin, Berlin, Germany. He is the Founding Director of the Center of Nanophotonics at Technical University of Berlin. He held guest professorships at the Technion, Haifa, Israel, the University of California at Santa Barbara, Santa Barbara, CA, USA, and Hewlett-Packard, Palo Alto, CA, USA. He was a Distinguished Adjunct Professor with King Abdulaziz University, Jeddah, Saudi Arabia, from 2012 to 2018, and the Einstein Professor with the Chinese Academy of Sciences in 2017 and 2018. Since 2018, he has been the Director of the Bimberg Chinese–German Center for Green Photonics, Chinese Academy of Sciences, Changchun Institute of Optics, Fine Mechanics, and Physics, Changchun, China. He authored more than 1600 papers, 71 patents, and six books. The numbers of times his research has been cited exceeds 68 000 and his Hirsch index is 113. His research interests include physics and technology of nanostructures, nanostructured photonic and electronic devices and energy efficient data communication. He is a member of the Russian Academy of Sciences and the German Academy of Sciences Leopoldina, a Foreign Member of the National Academy of Engineering of USA, and a Fellow of the U.S. National Institute of Inventors. The American Physical Society and IEEE elected him as Fellow/Life Fellow, respectively. Numerous international awards, such as the UNESCO award and medal for nanoscience and technology and the Russian State Prize for Science and Technology were bestowed to him. In 2020 he received the highest German award in experimental physics, the Stern–Gerlach medal.